https://doi.org/10.1016/j.scitotenv.2021.146241

Characteristics and source apportionment of volatile organic compounds (VOCs) at a coastal site in Hong Kong

Yan Tan [a], Shuwen Han [a], Yi Chen [a], Zhuozhi Zhang [a], Haiwei Li [b], Wenqi Li [a], Qi Yuan [a], Xinwei Li [a], Tao Wang [a], Shun-cheng Lee [a, *]

[a] *Department of Civil and Environmental Engineering, The Hong Kong Polytechnic University, Hong Kong, SAR of China*

[b] *Jiangsu Key Laboratory of Atmospheric Environment Monitoring and Pollution Control (AEMPC), Collaborative Innovation Center of Atmospheric Environment and Equipment Technology (CIC-AEET), School of Environmental Science and Engineering, Nanjing University of Information Science and Technology, Nanjing, 210044, China*

Correspondence authors:

Prof. Shun-cheng Lee, E-mail: shun-cheng@polyu.edu.hk, Telephone: +852 2766 6011

Graphical Abstract

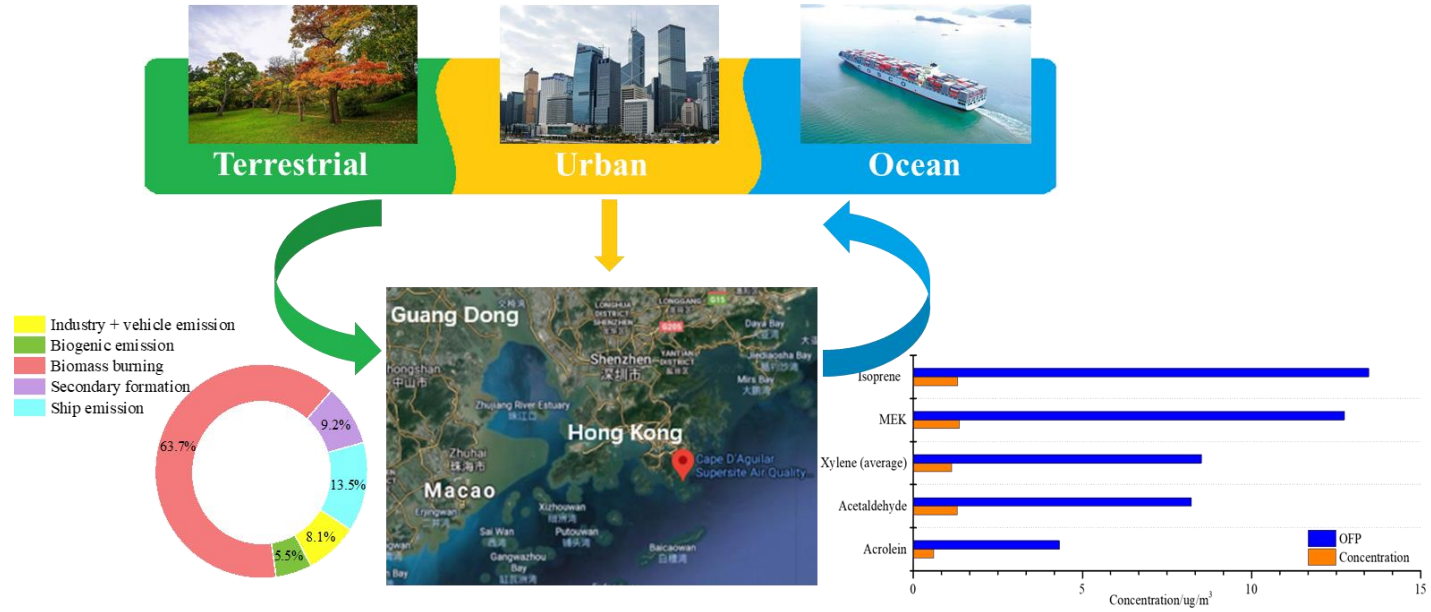

Highlights (for review : 3 to 5 bullet points (maximum 85 characters including spaces per bullet point)

Highlights

- VOCs concentrations were measured online by PTR-MS during autumn in Hong Kong.
- OVOCs were the dominant species with potential for ozone formation.
- The largest contributor to ambient VOCs was biomass burning during campaign.
- The air pollution in Hong Kong was strongly influenced by urban plumes from GBA/PRD and by oceanic emissions.

Abstract

Volatile organic compounds (VOCs) that are emitted from biomass burning, vehicle exhaust, and industrial emissions play a vital role in the formation of ozone (O_3) and secondary organic aerosols (SOA). Since VOCs are the precursors of O_3 and aerosol pollution which have become the world's most emergent environmental problems, a field measurement study focused on VOCs was carried out from 27 August to 10 October 2018 in a rural coastal site in Hong Kong. During the campaign, 13 VOC species were detected continuously with proton-transfer-reaction quadrupole mass spectrometry, and their effects on photochemical air pollution were studied. Methanol was the most abundant species among the measured VOCs (average concentration, 3.73 ± 3.26 ppb), and higher concentrations of oxygenated VOCs were found than reported in previous studies of atmospheric chemistry in rural areas. Diurnal variations were observed in the concentrations of various VOC species, indicating that the VOC concentrations were influenced by photochemical reactions. The amount of O_3 formation was estimated based on the maximum incremental reactivity scale of the VOCs. The top five contributors to O_3 formation in Hong Kong (in order) were isoprene (13.46 μg/m^3), methyl ethyl ketone (12.74 μg/m^3), xylene (8.52 μg/m^3), acetaldehyde (8.22 μg/m^3), and acrolein (4.32 μg/m^3). Receptor model positive matrix factorization (PMF) was used to identify the dominant emission sources and evaluate their corresponding contributions to VOCs. Five major VOC sources were identified with the PMF method, including (1) industry and vehicle-related sources (8.1%), (2) biogenic emissions (5.5%), (3) biomass burning (63.7%), (4) secondary formation

(9.2%), and (5) ship-related emissions (13.5%). The source apportionment results from PMF analysis show that the sampling site at the southeastern tip of Hong Kong was strongly influenced by urban plumes from the Guangdong–Hong Kong–Macao Greater Bay Area/Pearl River Delta region and by oceanic emissions.

Key Words: Volatile organic compounds (VOCs); Ozone formation potential (OFP); Source apportionment; PMF model; PTR-MS

1. Introduction

Volatile organic compounds (VOCs) are typical air pollutants, and many are carcinogenic (Loh et al., 2007; Stolwijk, 1990) and adversely affect human health (Azuma et al., 2016). In addition to these direct harmful effects on the human body, VOCs also exert significant effects on the atmospheric chemistry. In the troposphere, VOCs oxidized by hydroxyl radicals (OH), ozone (O_3) and chlorine radical (Cl) radicals will generate intermediates such as hydroperoxy radicals (HO_2) and organic peroxy radicals (RO_2), causing the recycling of nitrogen oxides (NOx), and further influence photochemical processes (Claeys et al., 2004; Tham et al., 2016; Wang et al., 2016), especially the formation of the ground-level O_3 (Shao et al., 2009) and secondary organic aerosols (Yuan et al., 2013). It is thus crucial to identify and understand the characteristics of VOCs, as they are the precursors of photochemical smog and toxic species (Guo et al., 2007; Huang et al., 2015; Sun et al., 2018; Wang and Milford, 2001; Yen and Horng, 2009).

The Guangdong–Hong Kong–Macao Greater Bay Area (GBA) was defined in 2017 as including Hong Kong, Macao, and several municipal regions in Guangdong province, namely Guangzhou, Shenzhen, Zhuhai, Foshan, Huizhou, Dongguan, Zhongshan, Jiangmen, and Zhaoqing. With the Pearl River Delta region as its basis, the GBA will become a first-class international bay area and world-class urban agglomeration, but rapid industrialization and urbanization have led to many air pollution episodes. For example, the O_3 concentration on China's southern coast increased at a rate of 0.35 ppbv per year between 1994 and 2018 (Wang et al., 2019). Due to its high population density and its unique location in the southeast of the GBA, Hong Kong has also struggled with this large increase in VOC emissions (Chan et al., 2002; Cui et al., 2018; Lee et al., 2002) and O_3 pollution (So and Wang, 2003; Wang et al., 2017).

Studies have identified complex VOC sources and contributions in Hong Kong (Guo et al., 2007; Lau et al., 2010; Liu et al., 2008), which is a major metropolis south of China (Chan and Yao, 2008). Hong Kong's air quality is affected by its large population (7.5 million residents) and heavy traffic (nearly 880,000 registered vehicles). Emissions from solvents and vehicles are the key contributors to O_3 formation in the urban area of Hong Kong (Lam et al., 2013; Lau et al., 2010; Ling and Guo, 2014). Hong Kong is also affected by the Asian monsoon, which comprises marine wind from the southwest in summer and continental wind from the northeast in winter. The northern winds from the continent also reduce the air quality in autumn and winter (Lyu et al., 2020).

In general, the O_3 formation potential (OFP) reflects the contribution of VOC species to O_3 generation, and may be used to evaluate the key VOC species in O_3 episodes.

Identifying and quantifying the contributions from each source is also crucial for air pollution abatement and for the formulation of control measures and strategies. Positive matrix factorization (PMF) is one of the receptor models, which has been widely used to study the source VOC profiles (Anderson et al., 2001; Brown et al., 2007; Cai et al., 2010; Guo et al., 2011; Zhu et al., 2018). It is crucial to understand the chemical composition of VOCs, identify major source regions of air pollution, and quantify the relative contribution of each source sector to ambient VOC concentrations, especially for cities such as Hong Kong that experience severe photochemical smog and O_3 pollution.

In this study, field measurements were conducted at a coastal site (Hok Tsui; HT) in Hong Kong from August to October 2018. The VOC concentrations were measured using an online high-resolution instrument (proton-transfer-reaction quadrupole mass spectrometry; PTR-QMS). The concentrations of the 13 calibrated species of VOCs and oxygenated VOCs (OVOCs) were determined and thoroughly analyzed. The OFP was used to identify the key species for O_3 generation at the HT site, and PMF was used to apportion the VOCs to their respective sources. The updated source contributions were identified and quantified in Hong Kong and the GBA according to the PMF estimation results.

2. Methods

2.1 Sampling site and periods

The field measurements of VOCs were conducted at the Cape D'Aguilar Supersite Air-Quality Monitoring Station (the HT site; owned by the Hong Kong Environmental

Protection Department; 22.22°N, 114.25°E, 60 m above sea level), located at the southeastern tip of Hong Kong Island (**Fig. 1**). During autumn, the average temperature is 26.7°C, the average relative humidity is 72.5%, and it has a typical subtropical monsoon climate. As a rural coastal site that faces the South China Sea with a sea view of more than 270°, the HT site is usually an upwind corner of Hong Kong and the GBA and is strongly influenced by oceanic emissions, urban plumes, and biogenic emissions (Wang et al., 2009). Although this station is located in Hong Kong, the HT site has been widely used as an ideal regional background site to investigate air pollution in the GBA and Hong Kong region (Lee et al., 2002; Lui et al., 2017). The field campaigns were conducted during late summer and autumn in 2018 from 27 August to 10 October, which is a common period of photochemical and particulate pollution in Hong Kong and the GBA (Lyu et al., 2020). An extremely powerful and catastrophic tropical cyclone, Typhoon Mangkhut, formed in early September 2018 and caused extensive damage in Hong Kong and GBA in middle-to-late September 2018 (Cheung and Su, 2018). Hence, for safety reasons data for trace gases and VOCs were not obtained for 15–19 September and 17–25 September, respectively.

2.2 Measurement

For the first time, state-of-the-art high-resolution PTR-QMS (PTR-QMS 500, IONICON Analytik, Austria) was used to comprehensively investigate the photochemical oxidation of VOCs and the formation of secondary organic aerosols at a regional urban background site in Hong Kong. PTR-MS has been widely used for online VOC measurements in field studies (Li et al., 2019; Yuan et al., 2013b). In

principle, the continuous introduced VOCs which are injected into the drift tube via a Venturi-type inlet undergoes non-dissociative proton transfer from H_3O^+ ions (from water vapor via hollow cathode discharge) and further ionized as $VOC{\cdot}H^+$ fragments and then detected by a quadrupole mass filter (Hewitt et al., 2003). Normally, PTR-MS can only detect the substance with a proton affinity greater than water (165.2 kcal/mol). During this campaign, the PTR-MS operation system was operated under H_3O^+ mode, and H_3O^+ primary ions were set to a constant drift tube pressure of 2.2 mbar. The field density ratio (E/N; where E is the electric-field strength, and N is the gas-number density) was 136 Td, and the temperatures of the inside and outside sample inlets were both 60°C. The sampling flow-rate was 300 mL min^{-1} for the inlet flow controller and 245 mL min^{-1} for the pressure controller.

A large variety of VOCs and OVOCs were quantified online with PTR-MS at a high time resolution. The specific species of interest in this study were (1) alkenes, namely *m/z* 69 for isoprene and *m/z* 137 for monoterpenes; (2) aromatic hydrocarbons, namely *m/z* 79 for benzene, *m/z* 93 for toluene, and *m/z* 107 for xylene; (3) OVOCs, namely *m/z* 33 for methanol, *m/z* 45 for acetaldehyde, *m/z* 57 for acrolein, *m/z* 59 for acetone, *m/z* 71 for methyl vinyl ketone (MVK) and methacrolein (MACR), *m/z* 73 for methyl ethyl ketone (MEK), and *m/z* 113 for products from the ozonolysis of terpenes; and (4) others, such as *m/z* 42 for acetonitrile. The data were collected and processed with PTR-MS Viewer version 3.2. The signal of *m/z* 113 was observed in ambient air above a Ponderosa pine forest canopy in California, and the results from chamber experiments confirmed that this ion is consistent with the products of terpene ozonolysis (Lee et al.,

2006). Another field study at Mount Tai in China also identified the signal as representing unsaturated aldehydes or ketones (Inomata et al., 2010). As a result, we attributed this *m/z* 113 signal to the products from the ozonolysis of terpenes (terpenes oxidation products; TOPs). The PTR-MS program measured the above-mentioned *m/z* values at a time interval of approximately 26 s.

During the campaign, the ambient temperature changed slightly and humidity change contributed little on the major uncertainty in PTR-MS measurements (Eerdekens et al., 2009; Kari et al., 2018; Warneke et al., 2001). For quality control, the PTR-MS was calibrated with a gas calibration unit (GCU, IONICON Analytik, Austria) containing a standard gas canister (RESTEK canister, IONICON Analytik, Austria) containing 27 types of VOCs. Zero air was introduced every day, to check the baseline of VOCs. Calibration was conducted every week, and a five-point curve was used to qualify the concentrations of VOCs. The details of the calibration procedure, including the mixing ratio of the standard gas, the calibration curve, the correlation coefficient, and the detection limits, are listed in **Table S1**. All species observed during the field campaign had good correlation coefficients (0.995 to 0.997).

In addition, to integrate the VOC measurements, the concentrations of nitric oxide (NO), nitrogen dioxide (NO_2), O_3, carbon monoxide (CO), and sulfur dioxide (SO_2) were measured every minute. NO and NO_2 were measured with an NOx analyzer (Model 42i-TL, Thermo Fisher Scientific Inc., USA), and O_3 was measured with an O_3 analyzer (Model 49i, Thermo Fisher Scientific Inc., USA). CO was measured with an CO analyzer (Model 48i, Thermo Fisher Scientific Inc., USA), and SO_2 was measured with

177 an SO_2 analyzer (Model 43i, Thermo Fisher Scientific Inc., USA). The data for the CO
178 and SO_2 concentrations and for the meteorological conditions (temperature and relative
179 humidity) were provided by the Hong Kong Environmental Protection Department. The
180 sampling inlets of these trace gas analyzers were at the same position as those for PTR-
181 MS, and their flow-rates were 1.5 L min^{-1}. The time series of the above trace gases, the
182 meteorological conditions, and the representative biogenic VOC isoprene and
183 anthropogenic VOC benzene are shown in **Fig. 2**.

184 2.3 Ozone formation potential

185 VOCs are important precursors of ground-level ozone (Seinfeld et al., 2016). OFP is
186 extensively used to estimate the contribution of individual VOC compounds to O_3
187 generation (Huang et al., 2008), as it reflects the relative contribution of various VOCs
188 to the generation of O_3. The OFP was developed by implementing the box model
189 simulation with different scenarios, and the maximum incremental reactivity (MIR) is
190 used to reflect the ozone production which is more sensitive to the variation of VOCs
191 than NO_X. As a rural coastal site, the peak ozone concentration at HT is controlled by
192 both VOCs and NO_X in different seasons. But during the sample period, VOCs play a
193 more sensitive role in ozone formation (Jin and Holloway, 2015). In addition, the MIR
194 was also used for the estimation of OFP at HT (So and Wang, 2004) and Pearl River
195 Delta (PRD) rural areas (Tang et al., 2007) in previous studies. This is then used to
196 determine the key sources and precursors of O_3 ,and specific MIR and VOC
197 concentrations are used for OFP calculations, as follows (Equation (1)):

198 $$OFP\ (j) = Concentration(j) \times MIR(j) \quad (1)$$

where $OFP\ (j)$ is the OFP for the specific VOC species j; $Concentration(j)$ is the concentration of the VOC species j (in μg/m^3); and MIR (in grams of O_3 per gram of organic compound) is the maximum incremental reactivity coefficient of the VOC species j, as developed and obtained by Carter (Carter, 2010).

2.4 PMF for source apportionment

Source apportionment techniques generally use a receptor model based on intrinsic statistical features of ambient measurement data (Watson et al., 2001). The receptor model is used to estimate the source contributions of pollutions and to evaluate the bottom-up emission inventories, although these are difficult to establish due to significant uncertainties (Zhang et al., 2009). PMF is an advanced multivariate receptor model recommended by the United States Environmental Protection Agency (EPA), and is thus widely used for site-specific calculations of source profiles and the time series of these sources, including in cases where little is known about the source profiles (Brown et al., 2007; Cai et al., 2010; Guo et al., 2011; Huang et al., 2015; Yuan et al., 2012). EPA PMF version 5.0 was used in this field study to characterize and identify the sources of VOC species.

Theoretically, PMF presents the contribution of *n* chemical species from *p* independent sources with the following chemical mass equation (Miller et al., 1972):

$$x_{ij} = \sum_{k=1}^{p} g_{ik} f_{kj} + e_{ij} \quad (2)$$

where x_{ij} represents the concentration of j_{th} species in i_{th} chemical sample; g_{ik} represents the contribution of the k_{th} source to the ith sample; f_{kj} represents the score matrix of the j_{th} species on the k_{th} source factor; e_{ij} represents the residual

221 factor for the j_{th} species at the i_{th} chemical sample (Paatero, 1997), and p represents
222 the total number of independent sources, which is determined by several normalized
223 different factors, such as the residual distribution for a specific VOC sample, factor
224 scores of the measured concentrations of a VOC, and the error squares of concentration
225 for a specific VOC (Anderson et al., 2001). A minimized object function Q (see
226 Equation (3)) is introduced into this receptor model to yield the solution, which is based
227 on uncertainties (u).

228 $$Q = \sum_{i=1}^{m} \sum_{j=1}^{n} \left(\frac{e_{ij}}{s_{ij}}\right)^2 \quad (3)$$

229 where e_{ij} represents the residual factor for the j_{th} species at the ith chemical sample,
230 and s_{ij} represents the uncertainty of the j_{th} species at the i_{th} chemical sample, which
231 is calculated using the error fraction and method detection limit (Polissar et al., 1998).
232 Poirot et al. (2001) and Hopke (2014) have also developed methods to deal with data
233 that are missing or below the detection limit. The PMF model could extract source
234 contributions from ambient samples without source profile, source apportionment
235 rapidly.

236 **3. Results and discussion**

237 3.1 Observation of VOCs

238 **Table 1** shows the concentration of VOC species at the HT site and a comparison with
239 data from four other suburban sites: (1) Tai O (Guo et al., 2006), another coastal area
240 on the southwestern tip of Hong Kong; (2) Changdao (Yuan et al., 2013b), a coastal
241 area between Liaoning Peninsula and Jiaodong Peninsula; (3) the Panyu District of
242 Guangzhou (Zou et al., 2015), which is approximately 15 km south of downtown

Guangzhou (a key city in the GBA); and (4) the Huairou District of Beijing (Li et al., 2019), which is approximately 50 km from the North 5th Ring Road and influenced by the urban plume. The geographic locations of these sites are listed in **Fig. S1** in the Supplemental Information.

The range of average VOC concentrations measured at HT (0.07 ± 0.07 ppb [TOPs] to 3.73 ± 3.26 ppb [methanol]) was similar to that from other rural areas. However, slight differences existed in the concentration ranges of some species measured in these rural areas. For example, the average concentration of isoprene (a representative biogenic VOC (BVOC)) at the HT site was 0.47 ppb, which was similar to that at Tai O. Nevertheless, it is quite high relative to that at Changdao and Huairou. BVOCs play a critical role in the atmosphere and exert a great influence on climate (Fuentes et al., 2000); this has a significant effect on Hong Kong, a hot tropical city located downwind from dense forests (Guenther, 1995). The HT site is part of a marine reserve and is lush with native coastal plants; this large green area may generate high concentrations of isoprene. Besides, isoprene is also produced by marine organisms (Arnold et al., 2009; Broadgate et al., 2004; Tran et al., 2013) and it was detected in marine air by PTR-MS in southern Indian Ocean (Kameyama et al., 2014) and North Pacific Ocean (Kameyama et al., 2010). A study conducted on the CHINARE cruises suggested the existence of isoprene in the marine boundary layer and the importance of oceanic emissions to isoprene (Hu et al., 2013). As a result, the concentrations of MVK + MACR and MEK were also high, as they are the major intermediate products generated by isoprene oxidation. The same phenomenon was also observed in monoterpenes

commonly emitted from plants, whose concentration was approximately 1.9 times and 3.3 times than those measured at Changdao and Huairou, respectively.

Methanol was the most abundant species of the measured VOCs at HT (average concentration, 3.73 ± 3.26 ppb). The value was lower than that at Changdao, but similar to those reported in Barcelona (Filella and Peñuelas, 2006) and in Beijing, whose nearby areas of vegetation are similar to those of the HT site. Methanol mostly originated from biogenic emissions and secondary formation (from oxidation of methane). The dominant sink of methanol was reaction with atmospheric oxidants, such as OH radicals, NO_3 radicals, and O_3. The reactivities were low, which resulted in a relatively high concentration of methanol at the HT site (Atkinson, 2000). Acetone had the second-highest concentration observed during the HT campaigns (average concentration was 2.43 ± 1.43 ppb), which was slightly higher than the concentrations in Changdao (1.85 ppb) and Huairou (1.59 ppb). Similar to methanol, the major source of acetone was primary biogenic emissions, and it was consumed by photolysis and OH oxidation in the atmosphere. Although acetone showed less reactivity toward atmospheric oxidants than methanol, photodissociation still played an important role in its removal (Atkinson et al., 1999), which led to a lower concentration of acetone than methanol. Benzene, toluene, and xylene are the main components of aromatic VOCs. The average concentrations of these benzene series compounds (BTX) were lower than those in other rural sites. As the HT site is a background site of the GBA, the concentrations of VOCs measured at the HT site were typically lower than those found at the Changdao and Beijing rural sites (**Table 1**). However, some species were present

in high concentrations, which indicated the importance of BVOCs and the key role of photochemical oxidation on OVOCs formation at the HT site.

We previously conducted a study at the Mong Kok (MK) air quality monitoring station, a typical urban station in Hong Kong, using PTR-MS to characterize urban VOCs and OVOCs (Cui et al., 2016). **Fig. 3** shows a comparison of the VOC concentrations at suburban (HT) and urban (MK) sites and the suburban-to-urban ratios of the average concentrations for each compound. As shown in **Fig. 3(a)**, almost 80% of the measured VOCs concentrations at the HT site were lower than those that were previously recorded at the MK site. The blue line in **Fig. 3(b)** shows the average ratio (0.59) of the suburban and urban concentrations. In general, the concentrations of hydrocarbons were lower at the HT site than at the MK site because fewer emissions from vehicles and human activities were present at the former. The concentrations of the OVOCs acetone, MEK, and methanol were slightly higher at the HT site than those that were previously found at the MK site. As shown in **Fig. 3(b)**, the concentrations of methanol and acetone at the HT site were 1.13 times higher than those that were previously found at the MK site. Green plant emissions, including plant growth and decay, are reportedly the principal sources of methanol (Jacob et al., 2005; Schade et al., 2011). In addition, the differences in the meteorological conditions during these two campaigns may have led to an increase in the concentration of methanol. The measurement at the MK site was conducted during four different months (February, May, August and November 2013), thus the final obtained concentration was the average of the measurements from all four seasons. The lower temperature and weaker solar radiation during MK

measurements, especially during February and November (**Table S2**), may have led to a lower level of methanol formation from photochemical reactions. The concentration of MEK in suburban areas is 1.23 times higher than that in urban areas. In addition, the HT site is more than 90% covered by vegetation, which will lead to a high isoprene concentration and the generation of more isoprene-oxidation products in this area.

3.2 Diurnal variations

Fig. 4 shows the diurnal variations in VOC concentrations at the HT site. As shown in **Fig. 4**, the concentrations of all OVOCs were higher during the daytime than at nighttime, due to the solar radiation and higher temperature during the daytime, while there was no obvious peak in the concentrations of acetaldehyde and acrolein during the daytime. The presence of solar radiation and the higher temperature during the daytime facilitated the photochemical reactions that generate OVOCs, and thus the concentrations of the OVOCs peaked at noon. There were several minor peaks in methanol concentrations (e.g., at 05:00 and 12:00), which indicates that it had different sources. That 05:00 peak was most likely a result of dew formation. During this period, the increase in methanol was always accompanied by a reduction in the gap between the temperature and the dew point and by a low wind speed (**Fig. S2**), which indicates that methanol emissions were related to condensation; after the leaves became wet, methanol was dissolved and then released to the atmosphere. This phenomenon has also been described elsewhere (Filella and Peñuelas, 2006; Warneke et al., 1999). The noon peak in methanol concentration due to photochemical reaction was a result of the strongest solar radiation occurring at this point in the day. The concentration of acetone

showed a similar diurnal variation to methanol, without an effect from dew formation. There was a slight increase in the concentration of all OVOCs at night, which was attributed (except for acrolein) to the change in the boundary layer height. Aromatic compounds showed several maximum-concentration peaks throughout the day. The 07:00 peak was mainly due to the emissions from commuter traffic from a cable station near the site. The concentrations of benzene, toluene, and xylene decreased during the daytime due to reaction with OH radicals, but the differences in their loss ratios demonstrated the differences in their reaction rates (Seinfeld et al., 1998). Another peak around 20:00 was slightly later than the time of high emissions from normal rush-hour traffic, and thus may have been caused by long-distance transportation from the urban area. Isoprene and monoterpene concentrations exhibited the expected trend consistent with solar radiation, reached an apex at noon. The concentrations of MVK + MACR, the major photooxidation products of isoprene and monoterpene, and the products from the ozonolysis of terpenes, were greater in the afternoon because the accumulation of oxidated isoprene and monoterpene was lower at night. Acetonitrile, as an inert substance, reacts very slowly with OH radicals (Atkinson et al., 2008). There was a slight increase in the concentration of acetonitrile during the daytime, and a slow decrease after sunset. This curve was similar to that of acetonitrile concentration data from a rural site in New Hampshire, USA (Jordan et al., 2009), and was likely due to dry deposition (Talbot et al., 2005). The specific and detailed source apportionment for VOCs is discussed in Section 3.4.

3.3 Ozone formation potential of VOCs

353 Because VOCs are the precursors of O_3, it is important to evaluate their contribution to
354 O_3 formation The MIR method was developed to calculate and assess the contribution
355 of each VOC to total O_3 production (Carter, 1994). **Table 2** presents the OFP of the
356 VOC species measured at the HT site. The results indicate that the contributions of
357 alkanes, aromatic hydrocarbons, and OVOCs to O_3 formation were 26.54%, 20.45%,
358 and 53.02%, respectively, which indicates that OVOCs were the dominant species that
359 contributed to O_3 formation at the HT site. OVOCs have also been found to be the major
360 contributors to O_3 formation at rural sites rather than at urban sites (Luo et al., 2011).
361 The top five VOC species (in order) that contributed to O_3 formation were isoprene,
362 MEK, xylene, acetaldehyde, and acrolein (**Fig. 5**). Isoprene had the highest OFP (13.46
363 $\mu g/m^3$) of the measured VOCs, which accounted for 21.47% of the OFP of all measured
364 VOC species. Previous field studies showed that biogenic emissions remain major
365 contributors to O_3 formation if only isoprene is considered (Lu et al., 2010; Xie et al.,
366 2008).

367 3.4 Source identification

368 In this study, the receptor model PMF version 5.0 was used to analyze the measured
369 VOC data sets for the HT site. The VOC species measured with online PTR-MS (N=
370 2597) were used to base run into the PMF model. Factor numbers 2 to7 were explored
371 to resolve the best solution for the PMF results, and various random SEEDs points were
372 used to minimize the results for each factor number (Paatero, 1997). In an attempt to
373 generate rotational ambiguity, the fPeak values were changed from –3 to 3. To confirm
374 the optimal values of the sources, **Fig. S3** shows the trials of the theoretical Q value

375 with the function of factor sizes. The value of Q/Q_{exp} decreased by 31% from factor 2
376 to factor 3, and by 41% from factor 3 to factor 4. As the number of factors continued to
377 increase to 5, the value of Q/Q_{exp} changed from 1.51 (factor 4) to 1.14 (factor 5), and
378 the decrease was then not obvious. The additional factors in PMF decrease the Q/Q_{exp}
379 values gradually, and Q/Q_{exp} values should be approximately equal to the number of
380 degrees of freedom or the total number of data points (Guo et al., 2011). Finally, five
381 source factors were selected for our analysis of Q/Q_{exp} values.
382 **Fig. 6** shows the source profiles as the percentage of each species mapped in each
383 respective factor and in terms of source apportionment. Factor 1 comprised high
384 percentages of the aromatic hydrocarbons benzene (26.95%), toluene (89.22%), and
385 xylene (79.17%). Because the industrial use of benzene has been forbidden and toluene
386 is a common ingredient in solvents, the ratio of toluene to benzene (T/B) is a valuable
387 indicator for the identification of emission sources (Zhang et al., 2013). The T/B ratio
388 shows a wide range in various studies. Normally, a relatively high T/B value is observed
389 in a typical industrial area (Sahu et al., 2016; Tiwari et al., 2010), and the ratio would
390 decreases as the contribution of vehicle emissions increases (Sahu et al., 2020). When
391 the T/B ratio falls below 1, biomass burning is the dominant source of emissions (Liu
392 et al., 2008). **Fig. 7** presents a scatterplot of toluene to benzene; the T/B slope at the HT
393 site of factor 1 was 3.2, which fell between the range of industrial and roadside emission.
394 The 72-h backward trajectories indicate that winds from mainland China passed
395 through many cities on the ground during the high T/B period from 19:00 to 21:00 on
396 September 28 (**Fig. S4**). This result suggests that factor 1 may reflect the mix of

industrial and automotive emissions.

The major species of factor 2 were isoprene, comprising more than 80% of its total concentration, and its oxidation products (MVK + MACR). TOPs also contributed more than 20% of this factor. Moreover, factor 2 peaked during the afternoon and decreased at night, which formed a similar diurnal curve with biogenic signals due to photosynthesis. Therefore, factor 2 was related to biogenic emissions.

Factor 3 was dominated by CO (75.5%), benzene (56.13%), acetonitrile (47.4%), and OVOCs (acetone, acetaldehyde, MEK, and acrolein). CO is an excellent tracer of combustion emissions, which are discharged from various sources, such as biomass (Wu et al., 2016), industry (Taiwo et al., 2014), vehicles (Watson et al., 2001), and residences (Gros and Sciare, 2009). Acetonitrile is a typical marker of biomass burning (de Gouw et al., 2003; Li et al., 2014). To better explain the trend and correlation, **Fig. 8 (a)** illustrates the time series of acetonitrile and CO concentrations. As depicted in **Fig. 8 (a)**, these two pollutants showed similar concentration variations during the field study. The time at which acetonitrile and CO reached their peak concentrations was almost identical, and three notable peaks that occurred on September 28, October 4, and October 8 are framed by a green dashed line. **Fig. S5** shows the 72-h backward trajectories and fire plots when the concentrations of acetonitrile and CO clearly increased. This reveals the pathways of the air masses that accompanied large numbers of fire plots at the HT site, which came mainly from mainland China during the period of high acetonitrile/CO concentrations. The pollutants that are generated by biomass burning are likely transported to the HT site by the continental wind. Biomass burning

has been verified as the major contributor to benzene emissions (Andreae and Merlet, 2001; Liu et al., 2008), and large concentrations of OVOCs, such as acetone, acetaldehyde, acrolein, and methanol, are also generated by this process (Karl et al., 2007; Read et al., 2012). Also, acetone and MEK had a high contribution to this factor of 63.6% and 50.6%, respectively. A field study at a rural site in north China revealed that primary emissions such as biomass burning were also a significant source of some OVOCs, such as acrolein, acetone, and MEK (Zhang et al., 2020). Lyu also proved that biomass burning is the largest contributor of organic aerosols at the HT site when the wind comes from the continent (Lyu et al., 2020). Therefore, the VOC species in factor 3 resulted from biomass burning.

A positive correlation was found between factor 4 and secondary formed tracers O_X (O_3 + NO_2; correlation coefficient, R^2 = 0.59) (**Fig. 8 (b)**), and factor 4 was distinguished by its high percentage of oxidation products. For example, the percentages of oxidation products contributed by isoprene and terpenes were 48.51% and 51.26%, respectively. In addition, the diurnal variation in factor 4 showed a maximum concentration in the afternoon and early evening. Hence, the high concentration of OVOCs was attributed mainly to secondary formation in factor 4.

Factor 5 at the HT site was characterized by high percentages of SO_2, NO_2, and NO. SO_2 and NO_X are important constituents of the marine boundary layer (Davis et al., 2001). Because the HT site is a coastal corner with a sea view of more than 270°, **Fig. S6** demonstrates that the concentration of SO_2 increased as the wind originated from the seaside. Acrolein, which contributed 13% to factor 5, is released when biodiesel is

441 heated or burned (Stevens and Maier, 2008). Thus, factor 5 was primarily related to
442 shipping emissions.
443 Based on the discussion above, five factors were identified from the PMF results at the
444 HT site in Hong Kong. **Fig. 9** illustrates the contributions of the five major emission
445 sources to the measured VOC concentrations. Generally, the most significant source
446 was biomass burning, which contributed to 63.7% of the measured VOC concentrations.
447 The second-largest source was ship-related emissions, which accounted for 13.5% of
448 the measured VOC concentrations. Secondary formation, a mix of industrial and
449 vehicle emissions and biogenic emissions, contributed 9.2%, 8.1%, and 5.5% of the
450 measured VOC concentrations during the campaign, respectively.

451 **4. Conclusions**

452 The concentrations of VOCs and OVOCs were measured by PTR-MS during autumn
453 in Hong Kong and their emission characteristics, OFP, and relative contributions from
454 various sources were explored. Methanol was found to be the most abundant species
455 among the measured VOCs (average concentration, 3.73 ± 3.26 ppb). The concentration
456 of isoprene and MEK in HT was higher than that which was previously observed in
457 other rural studies, suggesting besides biogenic emissions, the distinct oceanic
458 emissions contribute to BVOCs as well. A VOC data set was collected to estimate the
459 OFP. According to the MIR method, the top five contributors to O_3 formation in Hong
460 Kong (in order) were isoprene, MEK, xylene, acetaldehyde, and acrolein, and isoprene
461 accounted for 21.47% of all measured VOC species. OVOCs were the dominant species
462 at the HT site with the potential for O_3 formation.

The receptor model PMF was also used to identify possible sources and to evaluate the dominant sources of emissions. Five factors were extracted to identify the sources of VOCs in Hong Kong, namely industrial and vehicle emissions (8.1%); biogenic emissions (5.5%), biomass burning (63.7%), secondary formation (9.2%), and ship emissions (13.5%). The results indicate that the air pollution in Hong Kong was strongly influenced by urban plumes from GBA/PRD and by oceanic emissions during autumn.

Acknowledgments

This work was supported by The National Key Research and Development Program of China (2016YFA0203000), The Research Grants Council of Hong Kong Government (Project No. T24/504/17), and The Environment and Conservation Fund of Hong Kong Government (Project No. ECF 63/2019). The authors would like to thank the University Research Facility for Chemical and Environmental Analysis (UCEA) of PolyU for equipment support, and the HKEPD for providing the trace gases and meteorological data, and Mr. Steven Poon for his help during campaign.

Reference

Anderson, M.J., Miller, S.L., Milford, J.B., 2001. Source apportionment of exposure to toxic volatile organic compounds using positive matrix factorization. J. Expo. Anal. Environ. Epidemiol. 11, 295–307. https://doi.org/10.1038/sj.jea.7500168

Andreae, M.O., Merlet, P., 2001. Emission of trace gases and aerosols from biomass burning. Global Biogeochem. Cycles 15, 955–966. https://doi.org/10.1029/2000GB001382

Arnold, S.R., Spracklen, D. V, Williams, J., Yassaa, N., Sciare, J., Bonsang, B., Gros, V., Peeken, I., Lewis, A.C., Alvain, S., Alvain, M., 2009. Evaluation of the global oceanic isoprene source and its impacts on marine organic carbon aerosol. Atmos. Chem. Phys. 9, 1253–1262. https://doi.org/10.5194/acp-9-1253-2009

Atkinson, R., 2000. Atmospheric chemistry of VOCs and NO(x). Atmos. Environ. 34, 2063–2101. https://doi.org/10.1016/S1352-2310(99)00460-4

Atkinson, R., Baulch, D.L., Cox, R.A., Crowley, J.N., Hampson, R.F., Hynes, R.G., Jenkin, M.E., Rossi, M.J., Troe, J., Wallington, T.J., 2008. Evaluated kinetic and photochemical data for atmospheric chemistry: Volume IV - Gas phase reactions of organic\newline halogen species. Atmos. Chem. Phys. 8, 4141–4496. https://doi.org/10.5194/acp-8-4141-2008

Azuma, K., Uchiyama, I., Uchiyama, S., Kunugita, N., 2016. Assessment of inhalation exposure to indoor air pollutants: Screening for health risks of multiple pollutants in Japanese dwellings. Environ. Res. 145, 39–49. https://doi.org/10.1016/j.envres.2015.11.015

Broadgate, W.J., Malin, G., Küpper, F.C., Thompson, A., Liss, P.S., 2004. Isoprene

and other non-methane hydrocarbons from seaweeds: A source of reactive hydrocarbons to the atmosphere. Mar. Chem. 88, 61–73. https://doi.org/10.1016/j.marchem.2004.03.002

Brown, S.G., Frankel, A., Hafner, H.R., 2007. Source apportionment of VOCs in the Los Angeles area using positive matrix factorization. Atmos. Environ. 41, 227–237. https://doi.org/10.1016/j.atmosenv.2006.08.021

Cai, C., Geng, F., Tie, X., Yu, Q., An, J., 2010. Characteristics and source apportionment of VOCs measured in Shanghai, China. Atmos. Environ. 44, 5005–5014. https://doi.org/10.1016/j.atmosenv.2010.07.059

Carter, W.P.L., 2010. Development of the SAPRC-07 Chemical Mechanism and Updated Ozone Reactivity Scales, Report to the California Air Resources Board, Contracts No. 03-318, 06-408, and 07-730.

Carter, W.P.L., 1994. Development of ozone reactivity scales for volatile organic compounds. J. Air Waste Manag. Assoc. 44, 881–899. https://doi.org/10.1080/1073161x.1994.10467290

Chan, C.K., Yao, X., 2008. Air pollution in mega cities in China. Atmos. Environ. https://doi.org/10.1016/j.atmosenv.2007.09.003

Chan, C.Y., Chan, L.Y., Wang, X.M., Liu, Y.M., Lee, S.C., Zou, S.C., Sheng, G.Y., Fu, J.M., 2002. Volatile organic compounds in roadside microenvironments of metropolitan Hong Kong. Atmos. Environ. 36, 2039–2047. https://doi.org/10.1016/S1352-2310(02)00097-3

Cheung, T., Su, X., 2018. Typhoon Mangkhut officially Hong Kong's most intense

storm since records began. SCMP 17 Sept.

Claeys, M., Graham, B., Vas, G., Wang, W., Vermeylen, R., Pashynska, V., Cafmeyer, J., Guyon, P., Andreae, M.O., Artaxo, P., Maenhaut, W., 2004. Formation of Secondary Organic Aerosols Through Photooxidation of Isoprene. Science (80-.). 303, 1173–1176. https://doi.org/10.1126/science.1092805

Cui, L., Wang, X.L., Ho, K.F., Gao, Y., Liu, C., Hang Ho, S.S., Li, H.W., Lee, S.C., Wang, X.M., Jiang, B.Q., Huang, Y., Chow, J.C., Watson, J.G., Chen, L.W., 2018. Decrease of VOC emissions from vehicular emissions in Hong Kong from 2003 to 2015: Results from a tunnel study. Atmos. Environ. 177, 64–74. https://doi.org/10.1016/j.atmosenv.2018.01.020

Cui, L., Zhang, Z., Huang, Y., Lee, S.C., Blake, D.R., Ho, K.F., Wang, B., Gao, Y., Wang, X.M., Louie, P.K.K., 2016. Measuring OVOCs and VOCs by PTR-MS in an urban roadside microenvironment of Hong Kong: Relative humidity and temperature dependence, and field intercomparisons. Atmos. Meas. Tech. 9, 5763–5779. https://doi.org/10.5194/amt-9-5763-2016

Davis, D.D., Grodzinsky, G., Kasibhatla, P., Crawford, J., Chen, G., Liu, S., Bandy, A., Thornton, D., Guan, H., Sandholm, S., 2001. Impact of ship emissions on marine boundary layer NOx and SO2 distributions over the Pacific Basin. Geophys. Res. Lett. 28, 235–238. https://doi.org/10.1029/2000GL012013

de Gouw, J.A., Warneke, C., Parrish, D.D., Holloway, J.S., Trainer, M., Fehsenfeld, F.C., 2003. Emission sources and ocean uptake of acetonitrile (CH3CN) in the atmosphere. J. Geophys. Res. Atmos. 108. https://doi.org/10.1029/2002jd002897

546 Eerdekens, G., Ganzeveld, L., De Arellano, J.V.G., Klüpfel, T., Sinha, V., Yassaa, N.,
547 Williams, J., Harder, H., Kubistin, D., Martinez, M., Lelieveld, J., 2009. Flux
548 estimates of isoprene, methanol and acetone from airborne PTR-MS
549 measurements over the tropical rainforest during the GABRIEL 2005 campaign.
550 Atmos. Chem. Phys. 9, 4207–4227. https://doi.org/10.5194/acp-9-4207-2009
551 Filella, I., Peñuelas, J., 2006. Daily, weekly, and seasonal time courses of VOC
552 concentrations in a semi-urban area near Barcelona. Atmos. Environ. 40, 7752–
553 7769. https://doi.org/10.1016/j.atmosenv.2006.08.002
554 Gros, V., Sciare, J., 2009. Volatile organic compounds source apportionment in Paris
555 in spring 2007, Geophysical Research Abstracts.
556 Guenther, A., 1995. A global model of natural volatile organic compound emissions.
557 J. Geophys. Res. 100, 8873–8892. https://doi.org/10.1029/94JD02950
558 Guo, H., Cheng, H.R., Ling, Z.H., Louie, P.K.K., Ayoko, G.A., 2011. Which
559 emission sources are responsible for the volatile organic compounds in the
560 atmosphere of Pearl River Delta? J. Hazard. Mater. 188, 116–124.
561 https://doi.org/10.1016/j.jhazmat.2011.01.081
562 Guo, H., So, K.L., Simpson, I.J., Barletta, B., Meinardi, S., Blake, D.R., 2007. C1-C8
563 volatile organic compounds in the atmosphere of Hong Kong: Overview of
564 atmospheric processing and source apportionment. Atmos. Environ. 41, 1456–
565 1472. https://doi.org/10.1016/j.atmosenv.2006.10.011
566 Guo, H., Wang, T., Blake, D.R., Simpson, I.J., Kwok, Y.H., Li, Y.S., 2006. Regional
567 and local contributions to ambient non-methane volatile organic compounds at a

polluted rural/coastal site in Pearl River Delta, China. Atmos. Environ. 40, 2345–2359. https://doi.org/10.1016/j.atmosenv.2005.12.011

Hewitt, C.N., Hayward, S., Tani, A., 2003. The application of proton transfer reaction-mass spectrometry (PTR-MS) to the monitoring and analysis of volatile organic compounds in the atmosphere. J. Environ. Monit. https://doi.org/10.1039/b204712h

Hopke, P.K., 2014. A GUIDE TO POSITIVE MATRIX FACTORIZATION Physico-chemical and toxicological characterization of electronic cigarette exposure View project A GUIDE TO POSITIVE MATRIX FACTORIZATION, researchgate.net.

Hu, Q.H., Xie, Z.Q., Wang, X.M., Kang, H., He, Q.F., Zhang, P., 2013. Secondary organic aerosols over oceans via oxidation of isoprene and monoterpenes from Arctic to Antarctic. Sci. Rep. 3, 1–7. https://doi.org/10.1038/srep02280

Huang, S., Shao, M., Lu, S., Liu, Y., 2008. Reactivity of ambient volatile organic compounds (VOCs) in summer of 2004 in Beijing. Chinese Chem. Lett. 19, 573–576. https://doi.org/10.1016/j.cclet.2008.03.029

Huang, Y., Ling, Z.H., Lee, S.C., Ho, S.S.H., Cao, J.J., Blake, D.R., Cheng, Y., Lai, S.C., Ho, K.F., Gao, Y., Cui, L., Louie, P.K.K., 2015. Characterization of volatile organic compounds at a roadside environment in Hong Kong: An investigation of influences after air pollution control strategies. Atmos. Environ. 122, 809–818. https://doi.org/10.1016/j.atmosenv.2015.09.036

Inomata, S., Tanimoto, H., Kato, S., Suthawaree, J., Kanaya, Y., Pochanart, P., Liu,

590 Y., Wang, Z., 2010. PTR-MS measurements of non-methane volatile organic
591 compounds during an intensive field campaign at the summit of Mount Tai,
592 China, in June 2006. Atmos. Chem. Phys. 10, 7085–7099.
593 https://doi.org/10.5194/acp-10-7085-2010
594 Jacob, D.J., Field, B.D., Li, Q., Blake, D.R., de Gouw, J., Warneke, C., Hansel, A.,
595 Wisthaler, A., Singh, H.B., Guenther, A., 2005. Global budget of methanol:
596 Constraints from atmospheric observations. J. Geophys. Res. D Atmos. 110, 1–
597 17. https://doi.org/10.1029/2004JD005172
598 Jin, X., Holloway, T., 2015. Spatial and temporal variability of ozone sensitivity over
599 China observed from the Ozone Monitoring Instrument. J. Geophys. Res. 120,
600 7229–7246. https://doi.org/10.1002/2015JD023250
601 Jordan, C., Fitz, E., Hagan, T., Sive, B., Frinak, E., Haase, K., Cottrell, L., Buckley,
602 S., Talbot, R., 2009. Long-term study of VOCs measured with PTR-MS at a
603 rural site in New Hampshire with urban influences. Atmos. Chem. Phys. 9,
604 4677–4697. https://doi.org/10.5194/acp-9-4677-2009
605 Kameyama, S., Tanimoto, H., Inomata, S., Tsunogai, U., Ooki, A., Takeda, S., Obata,
606 H., Tsuda, A., Uematsu, M., 2010. High-resolution measurement of multiple
607 volatile organic compounds dissolved in seawater using equilibrator inlet-proton
608 transfer reaction-mass spectrometry (EI-PTR-MS). Mar. Chem. 122, 59–73.
609 https://doi.org/10.1016/j.marchem.2010.08.003
610 Kameyama, S., Yoshida, S., Tanimoto, H., Inomata, S., Suzuki, K., Yoshikawa-Inoue,
611 H., 2014. High-resolution observations of dissolved isoprene in surface seawater

612 in the Southern Ocean during austral summer 2010-2011. J. Oceanogr. 70, 225–
613 239. https://doi.org/10.1007/s10872-014-0226-8
614 Kari, E., Miettinen, P., Yli-Pirilä, P., Virtanen, A., Faiola, C.L., 2018. PTR-ToF-MS
615 product ion distributions and humidity-dependence of biogenic volatile organic
616 compounds. Int. J. Mass Spectrom. 430, 87–97.
617 https://doi.org/10.1016/j.ijms.2018.05.003
618 Karl, T.G., Christian, T.J., Yokelson, R.J., Artaxo, P., Hao, W.M., A.Guenther, 2007.
619 The Tropical Forest and Fire Emissions Experiment: method evaluation of
620 volatile organic compound emissions measured by PTR-MS, FTIR, and GC from
621 tropical biomass burning. Atmos. Chem. Phys. 7, 5883–5897.
622 Lam, S.H.M., Saunders, S.M., Guo, H., Ling, Z.H., Jiang, F., Wang, X.M., Wang,
623 T.J., 2013. Modelling VOC source impacts on high ozone episode days observed
624 at a mountain summit in Hong Kong under the influence of mountain-valley
625 breezes. Atmos. Environ. 81, 166–176.
626 https://doi.org/10.1016/j.atmosenv.2013.08.060
627 Lau, A.K.H., Yuan, Z., Yu, J.Z., Louie, P.K.K., 2010. Source apportionment of
628 ambient volatile organic compounds in Hong Kong. Sci. Total Environ. 408,
629 4138–4149. https://doi.org/10.1016/j.scitotenv.2010.05.025
630 Lee, A., Goldstein, A.H., Keywood, M.D., Gao, S., Varutbangkul, V., Bahreini, R.,
631 Ng, N.L., Flagan, R.C., Seinfeld, J.H., 2006. Gas-phase products and secondary
632 aerosol yields from the ozonolysis of ten different terpenes. J. Geophys. Res.
633 Atmos. 111. https://doi.org/10.1029/2005JD006437

Lee, S.C., Chiu, M.Y., Ho, K.F., Zou, S.C., Wang, X., 2002. Volatile organic compounds (VOCs) in urban atmosphere of Hong Kong. Chemosphere 48, 375–382. https://doi.org/10.1016/S0045-6535(02)00040-1

Li, K., Li, J., Tong, S., Wang, W., Huang, R.J., Ge, M., 2019. Characteristics of wintertime VOCs in suburban and urban Beijing: Concentrations, emission ratios, and festival effects. Atmos. Chem. Phys. 19, 8021–8036. https://doi.org/10.5194/acp-19-8021-2019

Li, L., Chen, Y., Zeng, L., Shao, M., Xie, S., Chen, W., Lu, S., Wu, Y., Cao, W., 2014. Biomass burning contribution to ambient volatile organic compounds (VOCs) in the chengdu-chongqing region (CCR), China. Atmos. Environ. 99, 403–410. https://doi.org/10.1016/j.atmosenv.2014.09.067

Ling, Z.H., Guo, H., 2014. Contribution of VOC sources to photochemical ozone formation and its control policy implication in Hong Kong. Environ. Sci. Policy 38, 180–191. https://doi.org/10.1016/j.envsci.2013.12.004

Liu, Y., Shao, M., Fu, L., Lu, S., Zeng, L., Tang, D., 2008. Source profiles of volatile organic compounds (VOCs) measured in China: Part I. Atmos. Environ. 42, 6247–6260. https://doi.org/10.1016/j.atmosenv.2008.01.070

Loh, M.M., Levy, J.I., Spengler, J.D., Houseman, E.A., Bennett, D.H., 2007. Ranking cancer risks of organic hazardous air pollutants in the United States. Environ. Health Perspect. 115, 1160–1168. https://doi.org/10.1289/ehp.9884

Lu, K., Zhang, Y., Su, H., Brauers, T., Chou, C.C., Hofzumahaus, A., Liu, S.C., Kita, K., Kondo, Y., Shao, M., Wahner, A., Wang, J., Wang, X., Zhu, T., 2010.

Oxidant (O3 + NO2) production processes and formation regimes in Beijing. J. Geophys. Res. Atmos. 115, D07303. https://doi.org/10.1029/2009JD012714

Lui, K.H., Ho, S.S.H., Louie, P.K.K., Chan, C.S., Lee, S.C., Hu, D., Chan, P.W., Lee, J.C.W., Ho, K.F., 2017. Seasonal behavior of carbonyls and source characterization of formaldehyde (HCHO) in ambient air. Atmos. Environ. 152, 51–60. https://doi.org/10.1016/j.atmosenv.2016.12.004

Luo, W., Wang, B., Liu, S., He, J., Jishu, C.W.-H.K. yu, 2011, U., 2011. VOC ozone formation potential and emission sources in the atmosphere of Guangzhou. Environ. Sci. Technol. (in Chinese) 24, 80–86.

Lyu, X., Guo, H., Yao, D., Lu, H., Huo, Y., Xu, W., Kreisberg, N., Goldstein, A.H., Jayne, J., Worsnop, D., Tan, Y., Lee, S.C., Wang, T., 2020. In Situ Measurements of Molecular Markers Facilitate Understanding of Dynamic Sources of Atmospheric Organic Aerosols. Environ. Sci. Technol. 54, 11058–11069. https://doi.org/10.1021/acs.est.0c02277

Miller, M.S., Friedlander, S.K., Hidy, G.M., 1972. A chemical element balance for the Pasadena aerosol. J. Colloid Interface Sci. 39, 165–176. https://doi.org/10.1016/0021-9797(72)90152-X

Paatero, P., 1997. Least squares formulation of robust non-negative factor analysis, in: Chemometrics and Intelligent Laboratory Systems. pp. 23–35. https://doi.org/10.1016/S0169-7439(96)00044-5

Poirot, R.L., Wishinski, P.R., Hopke, P.K., Polissar, A. V., 2001. Comparative application of multiple receptor methods to identify aerosol sources in northern

678 Vermont. Environ. Sci. Technol. 35, 4622–4636.
679 https://doi.org/10.1021/es010588p
680 Polissar, A. V., Hopke, P.K., Paatero, P., Malm, W.C., Sisler, J.F., 1998. Atmospheric
681 aerosol over Alaska 2. Elemental composition and sources. J. Geophys. Res.
682 Atmos. 103, 19045–19057. https://doi.org/10.1029/98JD01212
683 Read, K.A., Carpenter, L.J., Arnold, S.R., Beale, R., Nightingale, P.D., Hopkins, J.R.,
684 Lewis, A.C., Lee, J.D., Mendes, L., Pickering, S.J., 2012. Multiannual
685 observations of acetone, methanol, and acetaldehyde in remote tropical Atlantic
686 air: Implications for atmospheric OVOC budgets and oxidative capacity.
687 Environ. Sci. Technol. 46, 11028–11039. https://doi.org/10.1021/es302082p
688 Sahu, L.K., Pal, D., Yadav, R., Munkhtur, J., 2016. Aromatic VOCs at Major Road
689 Junctions of a Metropolis in India: Measurements Using TD-GC-FID and PTR-
690 TOF-MS Instruments. Aerosol Air Qual. Res. 16, 2405–2420.
691 https://doi.org/10.4209/aaqr.2015.11.0643
692 Sahu, L.K., Yadav, R., Tripathi, N., 2020. Aromatic compounds in a semi-urban site
693 of western India: Seasonal variability and emission ratios. Atmos. Res. 246.
694 https://doi.org/10.1016/j.atmosres.2020.105114
695 Schade, G.W., Solomon, S.J., Dellwik, E., Pilegaard, K., Ladstätter-Weissenmayer,
696 A., 2011. Methanol and other VOC fluxes from a Danish beech forest during late
697 springtime. Biogeochemistry 106, 337–355. https://doi.org/10.1007/s10533-010-
698 9515-5
699 Seinfeld, J.H., Pandis, S.N., Noone, K., 2016. Atmospheric Chemistry and Physics:

From Air Pollution to Climate Change, John Wiley & Sons. https://doi.org/10.1063/1.882420

Seinfeld, J.H., Pandis, S.N., Noone, K., 1998. Atmospheric Chemistry and Physics: From Air Pollution to Climate Change. Phys. Today 51, 88–90. https://doi.org/10.1063/1.882420

Shao, M., Zhang, Y., Zeng, L., Tang, X., Zhang, J., Zhong, L., Wang, B., 2009. Ground-level ozone in the Pearl River Delta and the roles of VOC and NOx in its production. J. Environ. Manage. 90, 512–518. https://doi.org/10.1016/j.jenvman.2007.12.008

So, K.L., Wang, T., 2004. C3-C12 non-methane hydrocarbons in subtropical Hong Kong: Spatial-temporal variations, source-receptor relationships and photochemical reactivity. Sci. Total Environ. 328, 161–174. https://doi.org/10.1016/j.scitotenv.2004.01.029

So, K.L., Wang, T., 2003. On the local and regional influence on ground-level ozone concentrations in Hong Kong. Environ. Pollut. 123, 307–317. https://doi.org/10.1016/S0269-7491(02)00370-6

Stevens, J.F., Maier, C.S., 2008. Acrolein: Sources, metabolism, and biomolecular interactions relevant to human health and disease. Mol. Nutr. Food Res. https://doi.org/10.1002/mnfr.200700412

Stolwijk, J.A.J., 1990. Assessment of Population Exposure and Carcinogenic Risk Posed by Volatile Organic Compounds in Indoor Air. Risk Anal. 10, 49–57. https://doi.org/10.1111/j.1539-6924.1990.tb01019.x

Sun, J., Shen, Z., Huang, Y., Cao, J., Ho, S.S.H., Niu, X., Wang, T., Zhang, Q., Lei, Y., Xu, H., Liu, H., 2018. VOCs emission profiles from rural cooking and heating in Guanzhong Plain, China and its potential effect on regional O₃ and SOA formation. Atmos. Chem. Phys. Discuss. 1–20. https://doi.org/10.5194/acp-2018-36

Taiwo, A.M., Harrison, R.M., Shi, Z., 2014. A review of receptor modelling of industrially emitted particulate matter. Atmos. Environ. https://doi.org/10.1016/j.atmosenv.2014.07.051

Talbot, R., Mao, H., Sive, B., 2005. Diurnal characteristics of surface level O3 and other important trace gases in New England. J. Geophys. Res. D Atmos. 110, 1–16. https://doi.org/10.1029/2004JD005449

Tang, J.H., Chan, L.Y., Chan, C.Y., Li, Y.S., Chang, C.C., Liu, S.C., Wu, D., Li, Y.D., 2007. Characteristics and diurnal variations of NMHCs at urban, suburban, and rural sites in the Pearl River Delta and a remote site in South China. Atmos. Environ. 41, 8620–8632. https://doi.org/10.1016/j.atmosenv.2007.07.029

Tham, Y.J., Wang, Z., Li, Q., Yun, H., Wang, W., Wang, X., Xue, L., Lu, K., Ma, N., Bohn, B., Li, X., Kecorius, S., Größ, J., Shao, M., Wiedensohler, A., Zhang, Y., Wang, T., 2016. Significant concentrations of nitryl chloride sustained in the morning: Investigations of the causes and impacts on ozone production in a polluted region of northern China. Atmos. Chem. Phys. 16, 14959–14977. https://doi.org/10.5194/acp-16-14959-2016

Tiwari, V., Hanai, Y., Masunaga, S., 2010. Ambient levels of volatile organic

compounds in the vicinity of petrochemical industrial area of Yokohama, Japan. Air Qual. Atmos. Heal. 3, 65–75. https://doi.org/10.1007/s11869-009-0052-0

Tran, S., Bonsang, B., Gros, V., Peeken, I., Sarda-Esteve, R., Bernhardt, A., Belviso, S., 2013. A survey of carbon monoxide and non-methane hydrocarbons in the Arctic Ocean during summer 2010. Biogeosciences 10, 1909–1935. https://doi.org/10.5194/bg-10-1909-2013

Wang, L., Milford, J.B., 2001. Reliability of optimal control strategies for photochemical air pollution. Environ. Sci. Technol. 35, 1173–1180. https://doi.org/10.1021/es001358y

Wang, T., Dai, J., Lam, K.S., Nan Poon, C., Brasseur, G.P., 2019. Twenty-Five Years of Lower Tropospheric Ozone Observations in Tropical East Asia: The Influence of Emissions and Weather Patterns. Geophys. Res. Lett. 46, 11463–11470. https://doi.org/10.1029/2019GL084459

Wang, T., Tham, Y.J., Xue, L., Li, Q., Zha, Q., Wang, Z., Poon, S.C.N., Dubé, W.P., Blake, D.R., Louie, P.K.K., Luk, C.W.Y., Tsui, W., Brown, S.S., 2016. Observations of nitryl chloride and modeling its source and effect on ozone in the planetary boundary layer of southern China. J. Geophys. Res. 121, 2476–2489. https://doi.org/10.1002/2015JD024556

Wang, T., Wei, X.L., Ding, A.J., Poon, C.N., Lam, K.S., Li, Y.S., Chan, L.Y., Anson, M., 2009. Increasing surface ozone concentrations in the background atmosphere of Southern China, 1994-2007. Atmos. Chem. Phys. 9, 6217–6227. https://doi.org/10.5194/acp-9-6217-2009

766 Wang, T., Xue, L., Brimblecombe, P., Lam, Y.F., Li, L., Zhang, L., 2017. Ozone
767 pollution in China: A review of concentrations, meteorological influences,
768 chemical precursors, and effects. Sci. Total Environ. 575, 1582–1596.
769 https://doi.org/10.1016/j.scitotenv.2016.10.081
770 Warneke, C., Karl, T., Judmaier, H., Hansel, A., Jordan, A., Lindinger, W., Crutzen,
771 P.J., 1999. Acetone, methanol, and other partially oxidized volatile organic
772 emissions from dead plant matter by abiological processes: Significance for
773 atmospheric HO(X) chemistry. Global Biogeochem. Cycles 13, 9–17.
774 https://doi.org/10.1029/98GB02428
775 Warneke, C., Van Der Veen, C., Luxembourg, S., De Gouw, J.A., Kok, A., 2001.
776 Measurements of benzene and toluene in ambient air using proton-transfer-
777 reaction mass spectrometry: Calibration, humidity dependence, and field
778 intercomparison. Int. J. Mass Spectrom. 207, 167–182.
779 https://doi.org/10.1016/S1387-3806(01)00366-9
780 Watson, J.G., Chow, J.C., Fujita, E.M., 2001. Review of volatile organic compound
781 source apportionment by chemical mass balance. Atmos. Environ.
782 https://doi.org/10.1016/S1352-2310(00)00461-1
783 Wu, R., Li, J., Hao, Y., Li, Y., Zeng, L., Xie, S., 2016. Evolution process and sources
784 of ambient volatile organic compounds during a severe haze event in Beijing,
785 China. Sci. Total Environ. 560–561, 62–72.
786 https://doi.org/10.1016/j.scitotenv.2016.04.030
787 Xie, X., Shao, M., Liu, Y., Lu, S., Chang, C.C., Chen, Z.M., 2008. Estimate of initial

isoprene contribution to ozone formation potential in Beijing, China. Atmos. Environ. 42, 6000–6010. https://doi.org/10.1016/j.atmosenv.2008.03.035

Yen, C.H., Horng, J.J., 2009. Volatile organic compounds (VOCs) emission characteristics and control strategies for a petrochemical industrial area in middle Taiwan. J. Environ. Sci. Heal. - Part A Toxic/Hazardous Subst. Environ. Eng. 44, 1424–1429. https://doi.org/10.1080/10934520903217393

Yuan, B., Hu, W.W., Shao, M., Wang, M., Chen, W.T., Lu, S.H., Zeng, L.M., Hu, M., 2013a. VOC emissions, evolutions and contributions to SOA formation at a receptor site in Eastern China. Atmos. Chem. Phys. Discuss. 13, 6631–6679. https://doi.org/10.5194/acpd-13-6631-2013

Yuan, B., Hu, W.W., Shao, M., Wang, M., Chen, W.T., Lu, S.H., Zeng, L.M., Hu, M., 2013b. VOC emissions, evolutions and contributions to SOA formation at a receptor site in Eastern China. Atmos. Chem. Phys. Discuss. 13, 6631–6679. https://doi.org/10.5194/acpd-13-6631-2013

Yuan, B., Shao, M., de Gouw, J., Parrish, D.D., Lu, S., Wang, M., Zeng, L., Zhang, Q., Song, Y., Zhang, J., Hu, M., 2012. Volatile organic compounds (VOCs) in urban air: How chemistry affects the interpretation of positive matrix factorization (PMF) analysis. J. Geophys. Res. Atmos. 117, n/a-n/a. https://doi.org/10.1029/2012JD018236

Zhang, F., Shang, X., Chen, H., Xie, G., Fu, Y., Wu, D., Sun, W., Liu, P., Zhang, C., Mu, Y., Zeng, L., Wan, M., Wang, Y., Xiao, H., Wang, G., Chen, J., 2020. Significant impact of coal combustion on VOCs emissions in winter in a North

China rural site. Sci. Total Environ. 720, 137617.
https://doi.org/10.1016/j.scitotenv.2020.137617

Zhang, Q., Streets, D.G., Carmichael, G.R., He, K.B., Huo, H., Kannari, A., Klimont, Z., Park, I.S., Reddy, S., Fu, J.S., Chen, D., Duan, L., Lei, Y., Wang, L.T., Yao, Z.L., 2009. Asian emissions in 2006 for the NASA INTEX-B mission. Atmos. Chem. Phys. 9, 5131–5153. https://doi.org/10.5194/acp-9-5131-2009

Zhang, Y., Wang, X., Barletta, B., Simpson, I.J., Blake, D.R., Fu, X., Zhang, Z., He, Q., Liu, T., Zhao, X., Ding, X., 2013. Source attributions of hazardous aromatic hydrocarbons in urban, suburban and rural areas in the Pearl River Delta (PRD) region. J. Hazard. Mater. 250–251, 403–411. https://doi.org/10.1016/j.jhazmat.2013.02.023

Zhu, H., Wang, H., Jing, S., Wang, Y., Cheng, T., Tao, S., Lou, S., Qiao, L., Li, L., Chen, J., 2018. Characteristics and sources of atmospheric volatile organic compounds (VOCs) along the mid-lower Yangtze River in China. Atmos. Environ. 190, 232–240. https://doi.org/10.1016/j.atmosenv.2018.07.026

Zou, Y., Deng, X.J., Zhu, D., Gong, D.C., Wang, H., Li, F., Tan, H.B., Deng, T., Mai, B.R., Liu, X.T., Wang, B.G., 2015. Characteristics of 1 year of observational data of VOCs, NOx and O3 at a suburban site in Guangzhou, China. Atmos. Chem. Phys. 15, 6625–6636. https://doi.org/10.5194/acp-15-6625-2015

Tables

Table 1

Average concentration of VOCs at HT site and comparison to other studies*.

VOCs species	This study	Tai O, coastal	Changdao, rural	Panyu, rural	Huairou, rural
Methanol	3.73 ± 3.26	N.A.	5.67 ± 4.80	N.A.	3.42 ± 2.58
Acetonitrile	0.20 ± 0.20	N.A.	0.21 ± 0.12	N.A.	0.11 ± 0.10
Acetaldehyde	0.72 ± 0.59	N.A.	0.63 ± 0.44	3.66	0.83 ± 0.57
Acrolein	0.26 ± 0.23	N.A.	N.A.	N.A.	N.A.
Acetone	2.43 ± 1.43	N.A.	1.85 ± 0.92	N.A.	1.59 ± 1.17
Isoprene	0.47 ± 0.47	0.43 ± 0.73	0.01 ± 0.01	N.A.	0.04 ± 0.04
MVK + MACR	0.11 ± 0.10	N.A.	N.A.	1.14	0.13 ± 0.13
MEK	0.46 ± 0.31	N.A.	0.35 ± 0.22	N.A.	0.38 ± 0.38
Benzene	0.29 ± 0.20	0.87 ± 0.92	0.55 ± 0.36	N.A.	0.91 ± 0.91
Toluene	0.25 ± 0.25	5.67 ± 7.13	0.57 ± 0.51	N.A.	0.73 ± 0.73
Xylene	0.26 ± 0.26	0.38 ± 0.57	N.A.	N.A.	N.A.
Terpenes oxidation products	0.07 ± 0.07	N.A.	N.A.	N.A.	N.A.
Monoterpenes	0.13 ± 0.12	N.A.	0.07 ± 0.06	N.A.	0.04 ± 0.04

N.A. – not available.

*The unit of concentration for all VOCs species is ppb.

Table 2

Ozone formation potential of VOCs species at HT.

VOCs	Concentration (ug/m^3)*	MIR (g O^3/g VOCs)	OFP (ug/m^3)
Methanol	4.89	0.65	3.18
Acetaldehyde	1.30	6.34	8.22
Acrolein	0.60	7.24	4.32
Acetone	5.77	0.35	2.02
Isoprene	1.31	10.28	13.46
MVK+MACR (average)	0.32	7.615	2.40
MEK	1.36	9.39	12.74
Benzene	0.93	0.69	0.64
Toluene	0.94	3.88	3.66
Xylene (average)	1.13	7.55	8.52
Terpenes products	0.32	1.1	0.35
Monoterpenes	0.72	4.38	3.17

*The concentrations are the average concentration of VOCs at HT site.

Reference

Cui, L., Zhang, Z., Huang, Y., Lee, S.C., Blake, D.R., Ho, K.F., Wang, B., Gao, Y., Wang, X.M., Louie, P.K.K., 2016. Measuring OVOCs and VOCs by PTR-MS in an urban roadside microenvironment of Hong Kong: Relative humidity and temperature dependence, and field intercomparisons. Atmos. Meas. Tech. 9, 5763–5779. https://doi.org/10.5194/amt-9-5763-2016

Tang, J.H., Chan, L.Y., Chan, C.Y., Li, Y.S., Chang, C.C., Liu, S.C., Wu, D., Li, Y.D., 2007. Characteristics and diurnal variations of NMHCs at urban, suburban, and rural sites in the Pearl River Delta and a remote site in South China. Atmos. Environ. 41, 8620–8632. https://doi.org/10.1016/j.atmosenv.2007.07.029

Figures

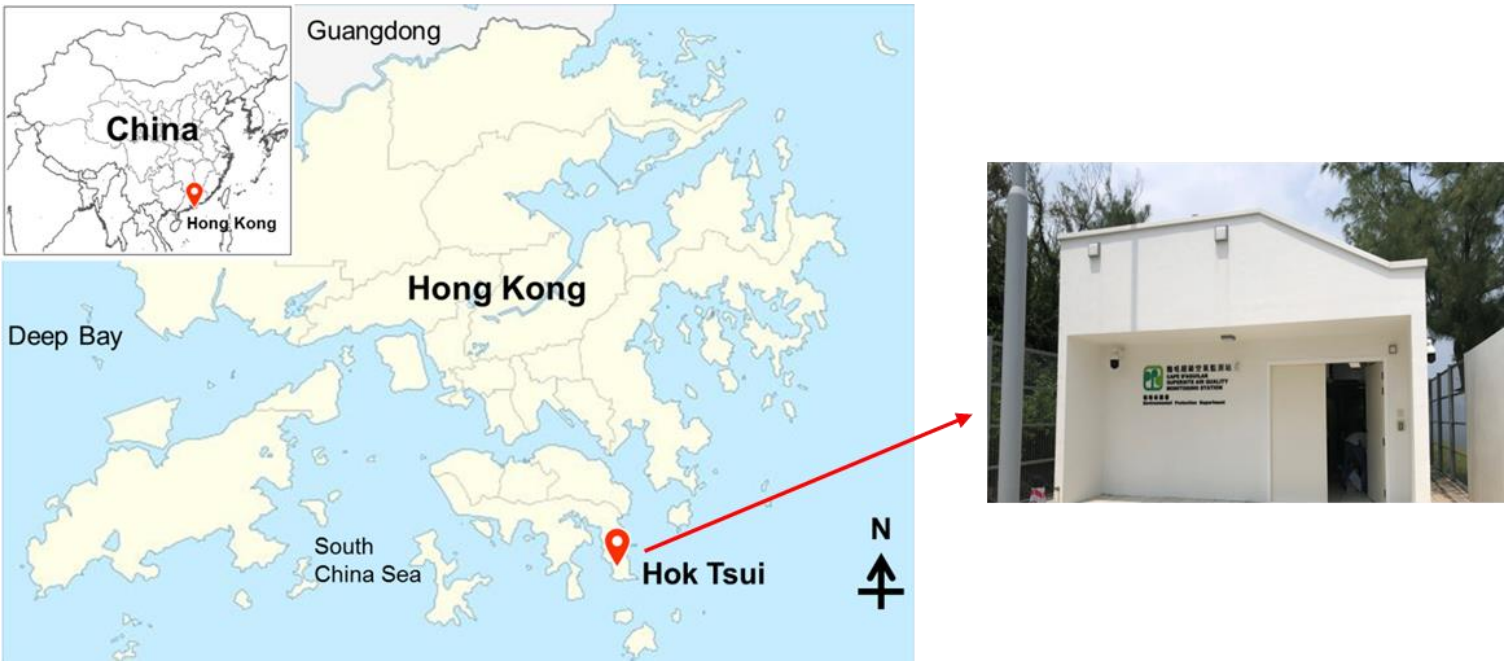

Fig. 1. Location and appearance of the sampling site in Hok Tsui (HT), Hong Kong

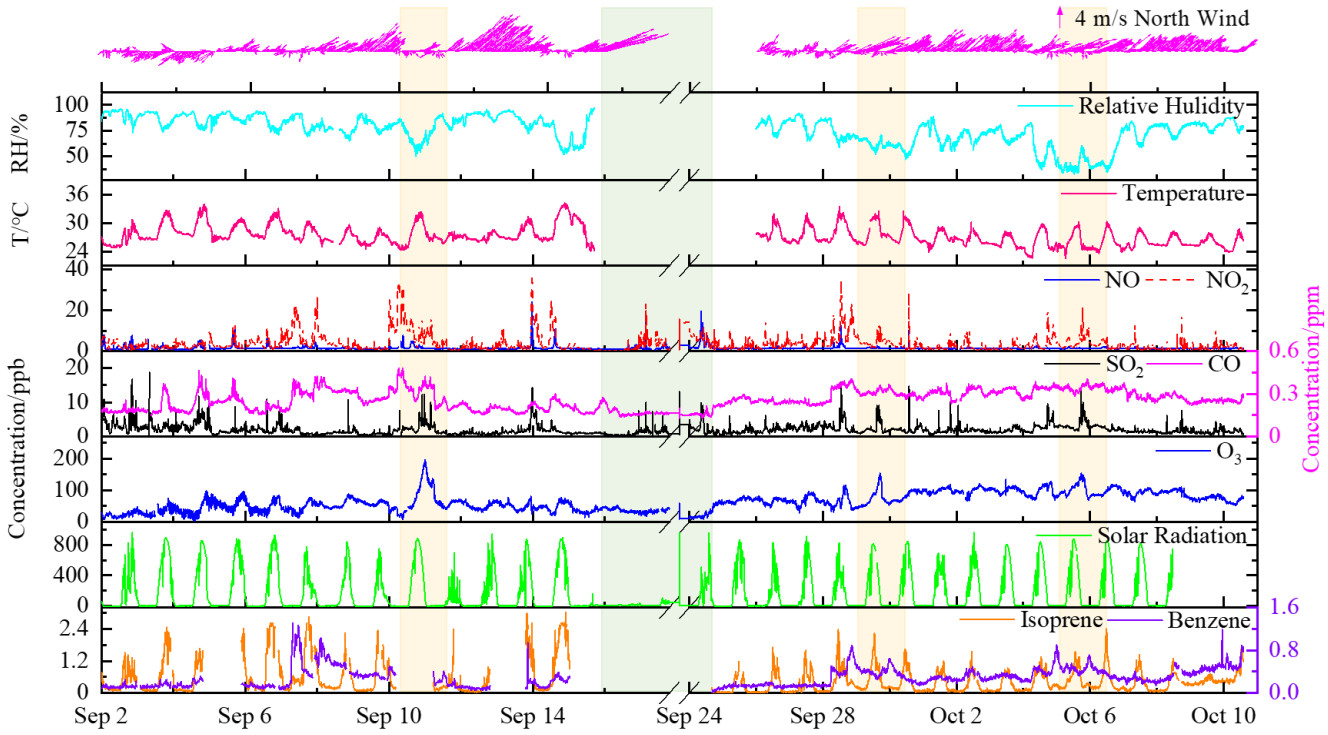

Fig. 2. Time series of meteorological parameters, SO_2, CO, O_3, NO_X and representative biogenic VOC isoprene and anthropogenic VOC benzene at the HT site. The yellow shaded-areas highlight the O_3 episodes; the green shaded-area marked as super typhoon Mangkhut landfall period.

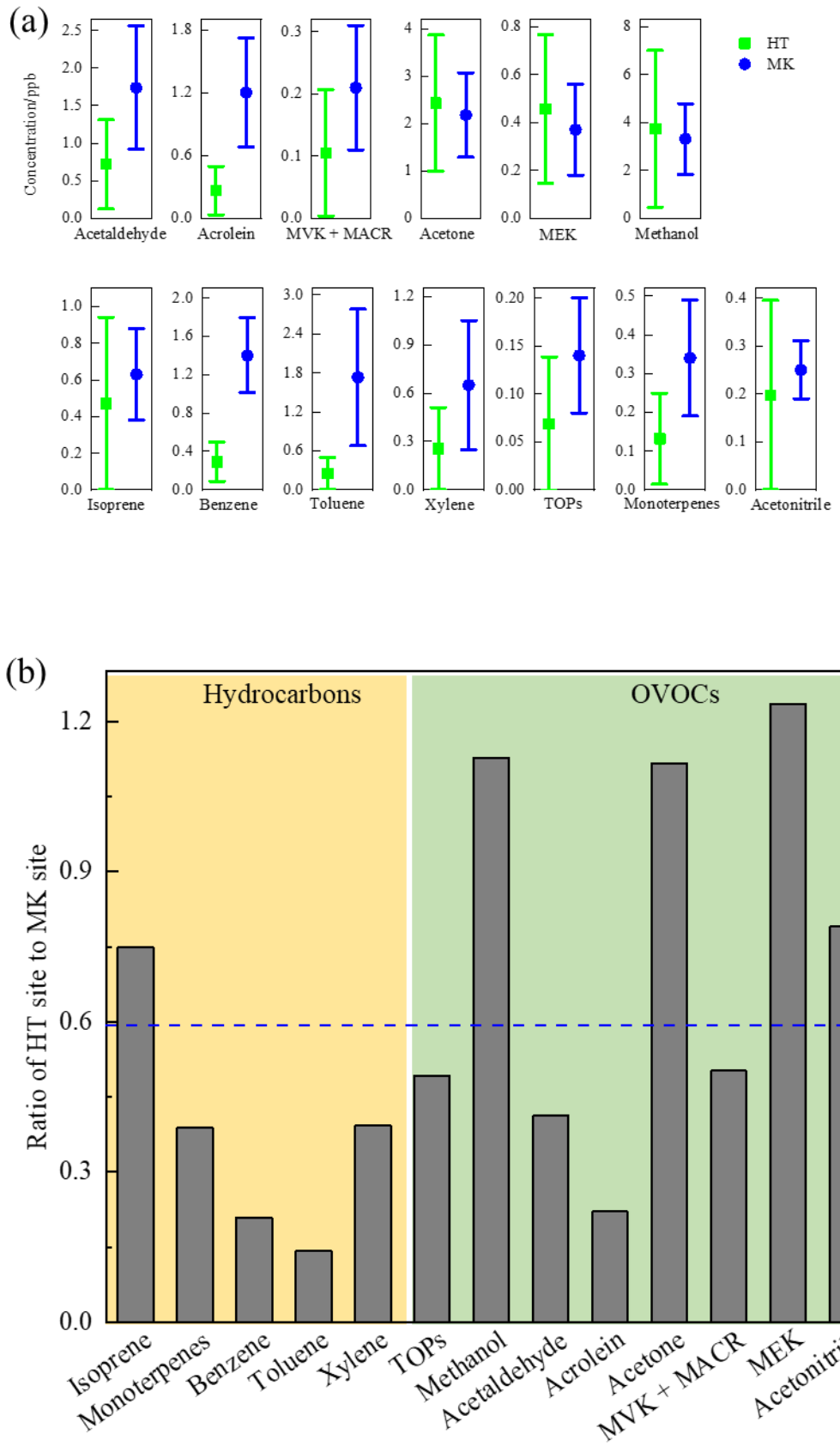

Fig. 3 Comparison of VOCs between coastal rural (HT) and urban (MK) sites: (a) the

average concentration of these two works, the solid squares are average concentration; the whiskers are standard deviation; (b) ratio of coastal rural site concentration to urban site concentration, the yellow shaded-area marks as hydrocarbon species, the green shaded-area marks as OVOCs species, the blue dot line is the average ratio value.

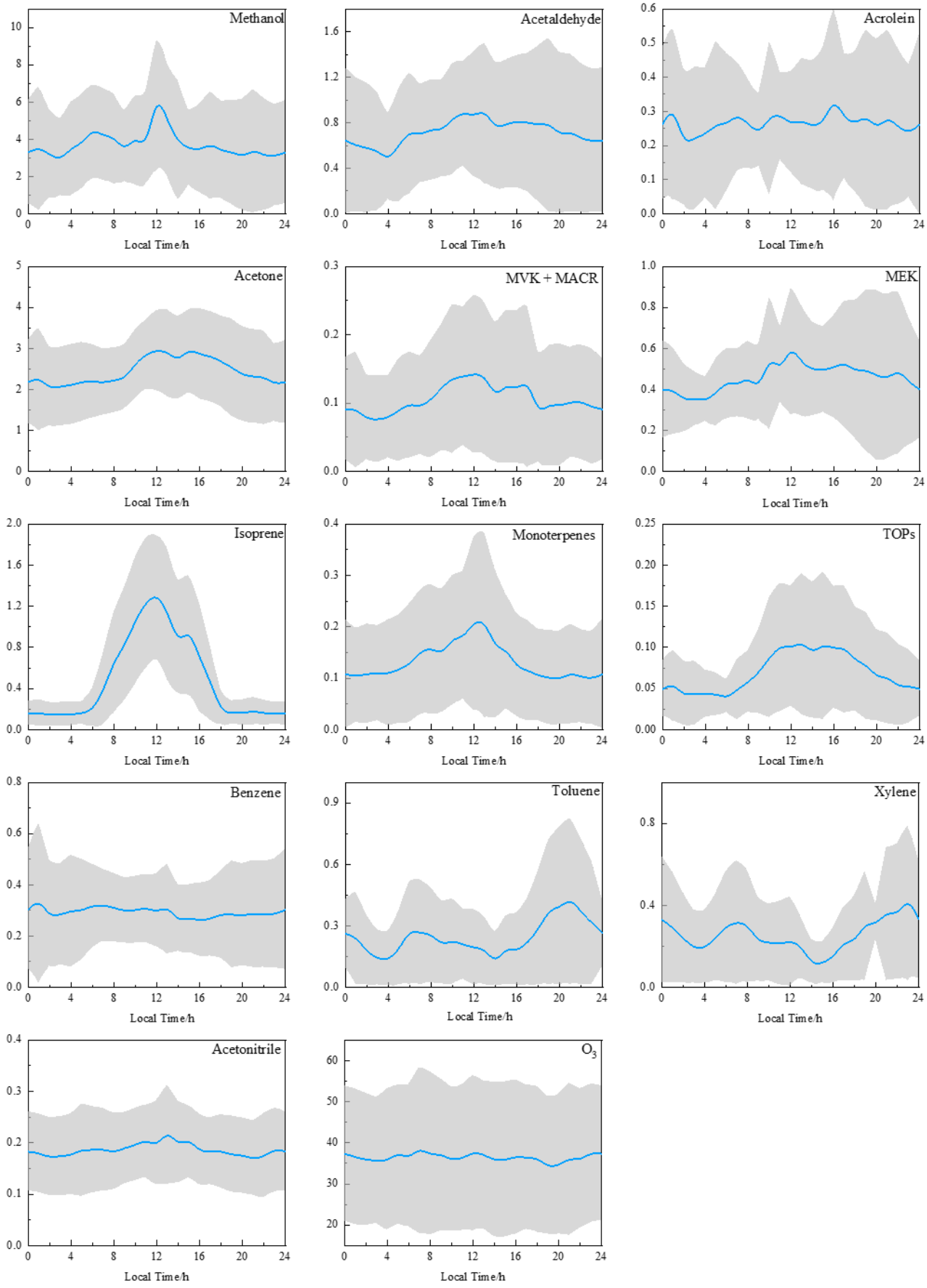

Fig. 4 Diurnal variations of VOCs and O_3 at HT site. The blue lines are average

concentrations, and gray areas indicate standard deviations. The unit of concentration for all VOCs species is ppb.

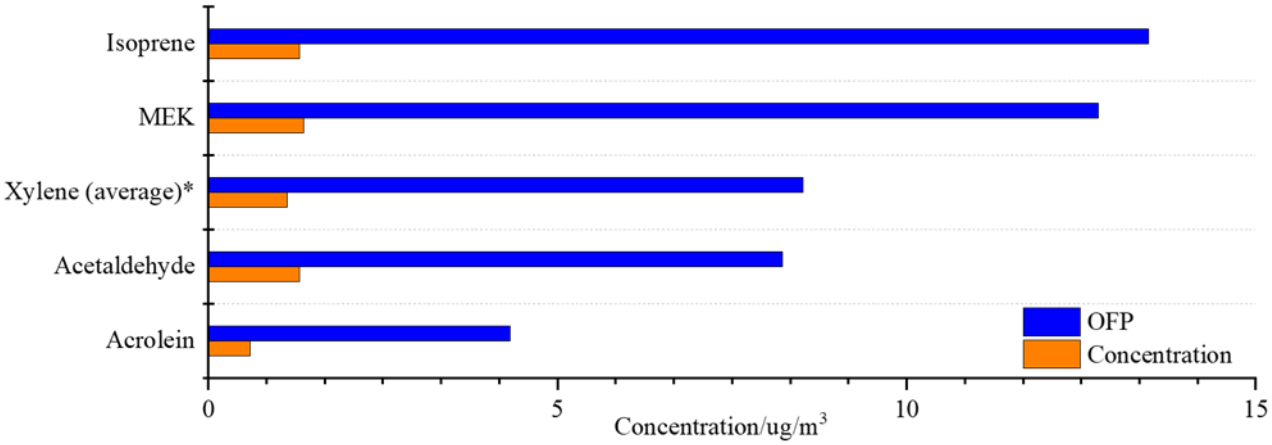

Fig. 5 Top five VOC species in emission concentration and corresponding OFP at HT site.

*Xylene is the arithmetic mean of m/p/o-xylene.

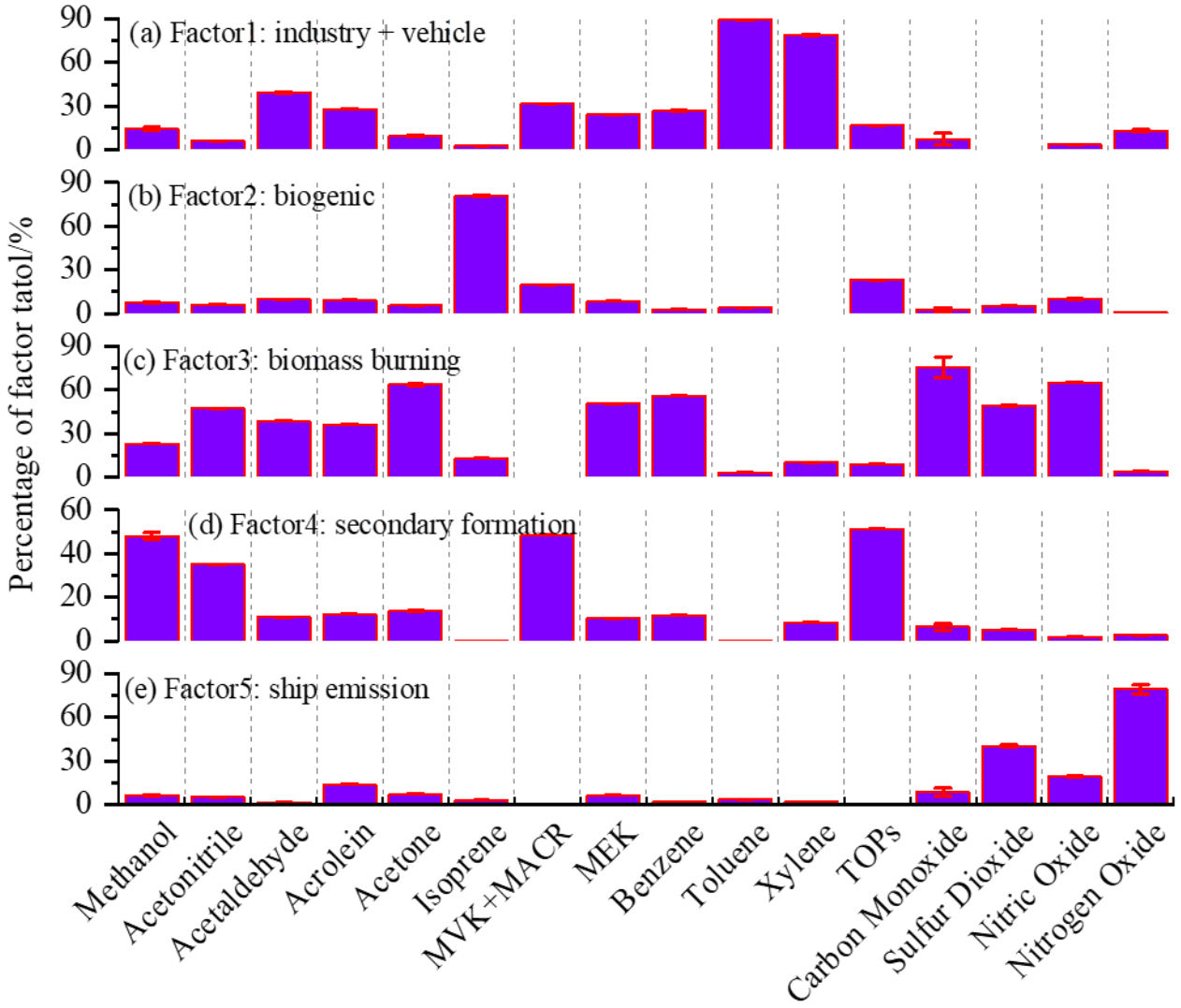

Fig. 6 Source profiles (percentage of factor total) resolved from PMF at HT site.

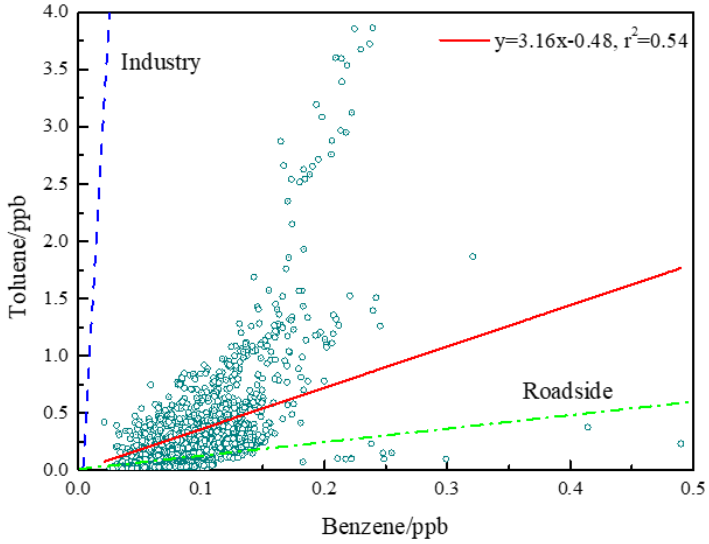

Fig. 7 Scatterplots of toluene to benzene at HT site in factor 1. Red line presents the T/B ratio in this study, blue dash line presents a study at Qingxi industrial township in Dong Guan, Guangdong province (Tang et al., 2007), green dash dot line presents a study from Mong Kok roadside station in Hong Kong (Cui et al., 2016).

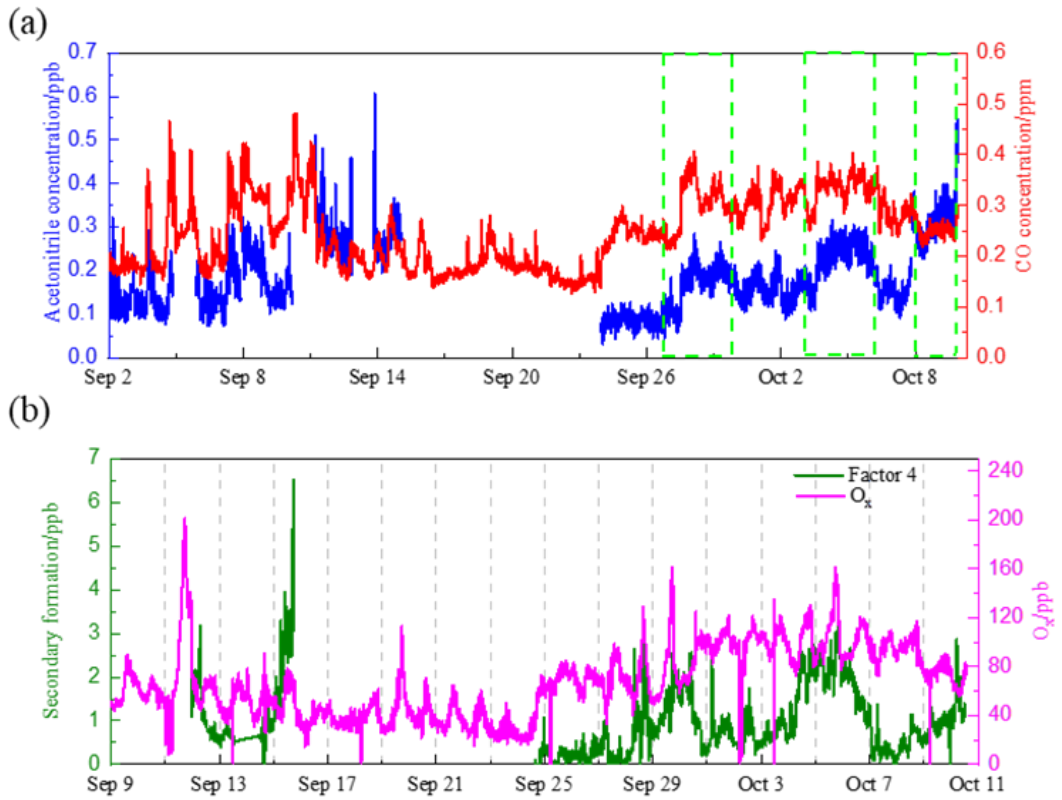

Fig. 8 Time series of (a) acetonitrile and CO, the green dash line circles three significant increases of acetonitrile and CO; (b) resolved factor 4 and O_X (O_3+NO_2) from PMF at HT site during campaign.

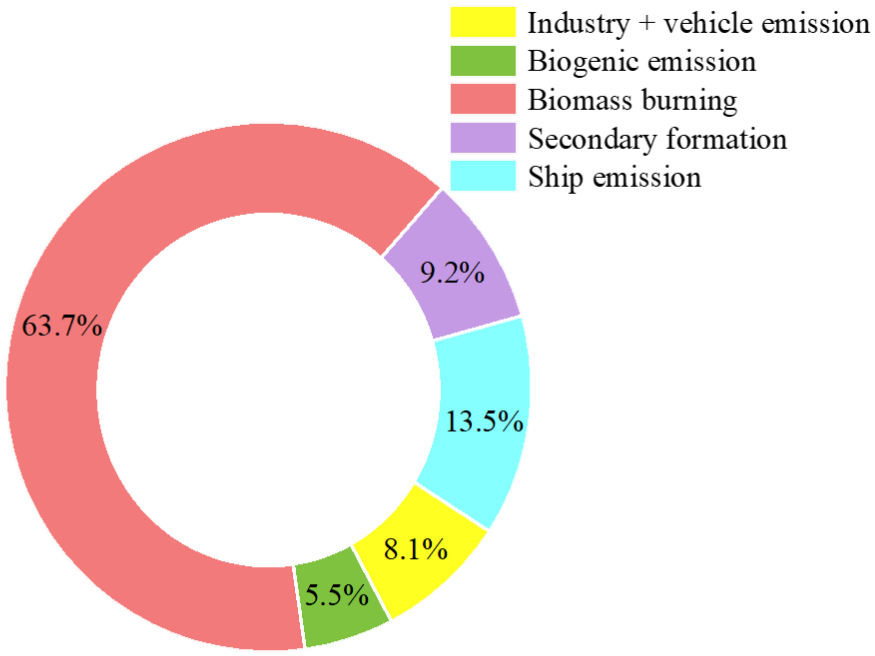

Fig. 9 Source apportionment results from PMF at HT site.

Reference

Cui, L., Zhang, Z., Huang, Y., Lee, S.C., Blake, D.R., Ho, K.F., Wang, B., Gao, Y., Wang, X.M., Louie, P.K.K., 2016. Measuring OVOCs and VOCs by PTR-MS in an urban roadside microenvironment of Hong Kong: Relative humidity and temperature dependence, and field intercomparisons. Atmos. Meas. Tech. 9, 5763–5779. https://doi.org/10.5194/amt-9-5763-2016

Tang, J.H., Chan, L.Y., Chan, C.Y., Li, Y.S., Chang, C.C., Liu, S.C., Wu, D., Li, Y.D., 2007. Characteristics and diurnal variations of NMHCs at urban, suburban, and rural sites in the Pearl River Delta and a remote site in South China. Atmos. Environ. 41, 8620–8632. https://doi.org/10.1016/j.atmosenv.2007.07.029

Credit Author Statement

Yan Tan: Writing - Original Draft, Investigation. **Shuwen Han:** Writing - Review & Editing, Investigation. **Yi Chen:** Writing - Review & Editing. **Zhuozhi Zhang:** Project administration. **Haiwei Li:** Project administration. **Wenqi Li:** Data Curation. **Qi Yuan:** Project administration. **Xinwei Li:** Project administration. **Tao Wang:** Funding acquisition, Project administration. **Shun-cheng Lee:** Supervision, Funding acquisition, Writing - Review & Editing.

Declaration of interests

☒ The authors declare that they have no known competing financial interests or personal relationships that could have appeared to influence the work reported in this paper.

☐The authors declare the following financial interests/personal relationships which may be considered as potential competing interests: